Review

Large Eddy Simulation as a Powerful Engineering Tool for Predicting Complex Turbulent Flows and Related Phenomena

Masahide Inagaki

Abstract

Computational Fluid Dynamics (CFD) has been applied in engineering predictions of turbulent fluid flow for about two decades. Above all, turbulence modeling is very important for predicting the performance of fluid machines with sufficient reliability since most of them involve complex turbulent phenomena. So far, the k-ε model has been most frequently used to predict various engineering turbulent flows with a certain degree of success. On the other hand, with the recent advances in computers, Large Eddy Simulation (LES) has become applicable to engineering prediction. The advantages of LES over the k-ε model are: (1) high prediction accuracy; (2) capability of resolving the unsteadiness of turbulent motion over a broad range of scales; (3) simplicity of modeling the turbulent effects in fluid phenomena containing multiphysics. For achieving the practical use of LES, we have developed a new subgrid-scale (SGS) model and a discretization method with high conservation property in curvilinear grids. The present paper provides descriptions thereof. In addition, the validity of LES using these techniques is investigated in some basic flows and engineering-relevant problems. LES is expected to become a powerful engineering tool for analyzing complex turbulent flows including heat and mass transfer, aerodynamic noise generation, combustion and so forth.

Keywords: Turbulence, Unsteady flow, Computational fluid dynamics, Aerodynamics, Aerodynamic noise, Large eddy simulation, Subgrid scale model

1. Introduction

Together with the recent remarkable advances in computers, numerical methods and turbulence modeling, Computational Fluid Dynamics (CFD) has become one of the most useful tools for investigating engineering application problems and designing fluid machinery. In automobile engineering, for example, such systems include external vehicle aerodynamics, the hydraulics for torque converters and spool valves, the air-conditioning system of the vehicle cabin and the in-cylinder flow of a reciprocating engine.

So far, the k-ε model has been most frequently used to predict such engineering turbulent flows. However, the k-ε model is not adequate to capture the unsteadiness of the turbulent flow itself over a broad range of scales because it is based on the Reynolds Averaged (time averaged) Navier-Stokes (RANS) equation. The characteristics of unsteady turbulent fluctuations are also important in many engineering applications, e.g., aerodynamic noise prediction, turbulent mixing and turbulent combustion in an engine. For resolving these complex turbulent flows and related phenomena, Large Eddy Simulation (LES) based on the space-filtered Navier-Stokes equation is a more suitable approach.

For utilizing LES for practical engineering applications, we have newly developed a subgrid-scale (SGS) model and a numerical method. In this paper, the proposed method and model are described, and the validity of LES using these techniques is investigated with respect to various aspects.

2. Numerical method

2. 1 Space-filtered basic equations

The velocity and pressure fields are decomposed into grid-scale (GS) components, $\overline{(\ )}$, and subgrid-scale (SGS) components, $(\ )'$:

$$u_i = \overline{u}_i + u_i', \quad p = \overline{p} + p' \qquad \cdots\cdots\cdots\cdots\cdots (1)$$

The GS component is defined by space filtering:

$$\overline{u}_i(x_1, x_2, x_3) = \int\!\!\int\!\!\int_{i=1}^{3} G_i(x_i, x_i', \Delta_i) \cdot u_i(x_1', x_2', x_3') dx_1' dx_2' dx_3' \cdots (2)$$

where the integral is extended over the entire flow field. G_i is a filtering function that serves to damp the spatial fluctuations with shorter length than the filter width, Δ_i. Typical filtering functions are the Gaussian filter, the cut-off filter and the top-hat filter. In practical use, a top-hat filter is applied because Gaussian or cut-off filters can be applied only in homogeneous directions. The basic equations are obtained by applying the filtering operation to the Navier-Stokes equation and the continuity equation as follows:

$$\frac{\partial \overline{u}_j}{\partial x_j} = 0 \qquad \cdots\cdots\cdots\cdots\cdots\cdots (3)$$

$$\frac{\partial \overline{u}_i}{\partial t} + \frac{\partial \overline{u}_j \overline{u}_i}{\partial x_j} = -\frac{1}{\rho}\frac{\partial \overline{p}}{\partial x_i} + \nu \frac{\partial \overline{u}_i}{\partial x_j^2} - \frac{\partial \tau_{ij}}{\partial x_j} \qquad \cdots\cdots\cdots (4)$$

where $\tau_{ij} = \overline{u_i u_j} - \overline{u}_i \overline{u}_j$ is the SGS stress tensor, which should be modeled. Here, flow is assumed to be incompressible.

2. 2 Subgrid-scale (SGS) modeling

2. 2. 1 Representative SGS models

The Smagorinsky model is a widely used SGS model, and is described as follows:

$$\tau_{ij} = -2\nu_t \overline{S}_{ij} + \frac{1}{3}\delta_{ij}\tau_{kk}, \quad \overline{S}_{ij} = \frac{1}{2}\left(\frac{\partial u_i}{\partial x_j} + \frac{\partial u_j}{\partial x_i}\right) \quad \cdots (5)$$

$$\nu_t = \left(Cs\overline{\Delta}f\right)^2 \left|\overline{S}\right|, \quad \left|\overline{S}\right| = \sqrt{2\overline{S}_{ij}\overline{S}_{ij}} \qquad \cdots\cdots\cdots (6)$$

where $\overline{\Delta} = (\Delta x \Delta y \Delta z)^{1/3}$. As a wall-damping function, f, van Driest's function is commonly used: $f_{VD} = 1 - \exp(-y^+/25)$. In this paper, a revised damping function[1], f_{PFM}, is also used.

When applied to simple flow fields, the Smagorinsky model is acknowledged to yield good results. However, the following are serious defects in practical application:

[1] The model must be supplemented with a proper wall-damping function of van Driest's type;

[2] The model parameter, C_S, needs to be adjusted according to the type of flow field;

[3] The SGS effect does not disappear in the laminar flow region.

The dynamic Smagorinsky model developed by Germano et al.[2] is an SGS model that overcomes these defects. In this model, the test filter is applied to the grid-filtered flow field. The sub-test-scale

stress is defined as $T_{ij} = \widetilde{\overline{u_i}\overline{u_j}} - \tilde{\overline{u}}_i \tilde{\overline{u}}_j$, where $\tilde{(\ )}$ denotes the test-filtering operator. By assuming the Smagorinsky model for both T_{ij} and τ_{ij}, the following relation is obtained:

$$L_{ij}^* = -2C\overline{\Delta}^2 M_{ij} \qquad \cdots\cdots\cdots\cdots\cdots\cdots (7)$$

where $L_{ij} = T_{ij} - \tilde{\tau}_{ij} = \widetilde{\overline{u_i}\overline{u_j}} - \tilde{\overline{u}}_i \tilde{\overline{u}}_j$, $C = (Csf)^2$, $M_{ij} = \alpha^2 \left|\tilde{\overline{S}}\right| \tilde{\overline{S}}_{ij} - \widetilde{\left|\overline{S}\right| \overline{S}_{ij}}$ and $\alpha = \tilde{\overline{\Delta}} / \overline{\Delta}$. The parameter C can be computed by applying a least-squares approach:

$$C = -\frac{1}{2} \frac{L_{ij}^* M_{ij}}{\overline{\Delta}^2 M_{ij} M_{ij}} \qquad \cdots\cdots\cdots\cdots\cdots (8)$$

Consequently, there is no need to give the model parameter or a wall-damping function beforehand. Namely, the defects of the Smagorinsky model are formally settled.

In spite of the remarkable success of the dynamic Smagorinsky model, some problems have occurred in its practical use. First, the obtained parameter C is not guaranteed to be positive, which leads to numerical instability. This restricts the time step allowing a stable calculation, which brings about an increase in computational cost. This is a great disadvantage in its practical use. Second, the accuracy is lower than that of the Smagorinsky model with the model parameter intentionally optimized for the relevant flow field.

2. 2. 2 Mixed-time-scale SGS model

To overcome the defects of the Smagorinsky model, we[3, 4] have proposed a new SGS model as follows:

$$\nu_t = C_{MTS} k_{SGS} T_S \qquad \cdots\cdots\cdots\cdots\cdots (9)$$

$$k_{SGS} = \left(\overline{u}_k - \hat{\overline{u}}_k\right)^2 \qquad \cdots\cdots\cdots\cdots\cdots (10)$$

$$T_S^{-1} = \left(\overline{\Delta} / \sqrt{k_{SGS}}\right)^{-1} + \left(C_T / \left|\overline{S}\right|\right)^{-1} \qquad \cdots\cdots\cdots (11)$$

The model parameters C_{MTS} and C_T are set to 0.05, and 10 respectively. $\hat{(\ )}$ denotes the filtering operator, for which the Simpson rule is adopted. In the estimation of the SGS kinetic energy, k_{SGS}, we employ the concept of scale similarity.[5] The essential point is that the time scale, T_s, is defined as the harmonic average of $\overline{\Delta} / \sqrt{k_{SGS}}$ and $1/\left|\overline{S}\right|$. The former is of primary importance and represents the characteristic time of the small scale motion corresponding to the cut-off scale, whereas the latter represents that of the large scales. The model performance is elucidated later.

2. 3 Modified 2nd-order collocated grid system

Since the GS components are directly computed, the prediction accuracy of LES depends on not only the SGS model but also on the discretization method. A discretization method with good conservation properties of mass, momentum and kinetic energy is desired because such good conservation properties make it possible to conduct a stable calculation with a central-difference scheme and dispense with employing an upwind finite-difference scheme that would probably contaminate the turbulent motion.

We have developed a 2nd-order collocated grid system,[6] which is modified from the original.[7] Owing to this modification, the new system has almost the same numerical accuracy as the 2nd-order staggered grid system which has a sufficient conservation property for LES, and which makes it possible to conduct LES in curvilinear grids with high stability and accuracy.

3. Assessment of SGS models in some basic flows

3. 1 Plane channel flow

To clarify the effectiveness of the present SGS model, we have performed an *a priori* test in a canonical channel flow.[3, 4] **Figure 1** shows the SGS eddy viscosity distribution calculated from each expression of the SGS model using the data of the

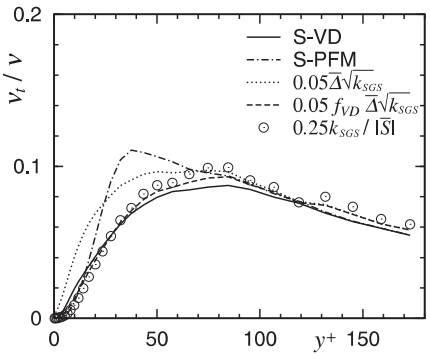

Fig. 1 *A priori* test for SGS eddy viscosity in channel flow (Case 1).

instantaneous flow field. In this figure, S-VD represents the Smagorinsky model with the wall-damping function, f_{VD} , and S-PFM is its revised version with f_{PFM} , where *Cs* is set to 0.1. Although the expression $k_{SGS}/|\overline{S}|$ is free from a damping function, it agrees well with other SGS models incorporated with a damping function. This result reveals that $1/|\overline{S}|$ is a proper time scale near the wall. To utilize the property of this time scale, we introduce the concept of the mixed time scale. A *posteriori* test[3, 4] proves that the present model does not need a wall-damping function supplemented.

3. 2 Backward-facing step flow

To verify the present SGS model in separating flows, we[3, 4] have applied it to the backward-facing step flow ($Re_H = 5{,}500$) corresponding to the experiment by Kasagi and Matsunaga.[8] In the Smagorimsky (S) model, *Cs* is set to 0.1, which is an optimized value for this flow field. For comparison with the standard dynamic Smagorinsky model (DS1 model) with $\gamma = \sqrt{3}$, the calculation using $\gamma = \sqrt{6}$ (DS2 model) is also conducted.

Figure 2 shows the Reynolds shear stress and the SGS eddy viscosity distributions. The dimensionless time step, Δt , allowing a stable calculation and the calculated flow reattachment length, X_R , are shown

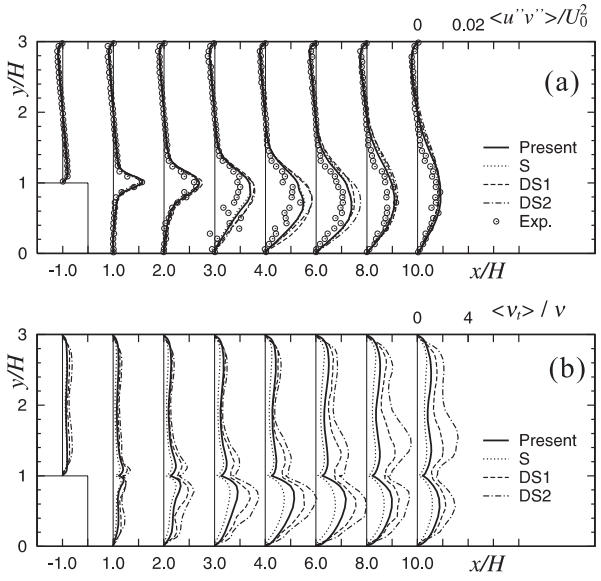

Fig. 2 Predictions of backward-facing step flow: (a) Reynolds shear stress; (b) SGS eddy viscosity.

in **Table 1**. The computational results obtained using the present model agree well with the experimental data, while the results obtained using DS1 or DS2 model show less accuracy and less computational stability. Owing to the computational instability, the time step in the calculation using the DS1 model must be set to about one-fourth of that using the S-VD model. On the other hand, the calculation using the present model is successfully performed with the same time step as in the calculation using the S-VD model. This computational stability is due to the fixed model-parameters that are employed instead of the dynamically adjusted model-parameters adopted in the dynamic model. By using the DS2 model, the restriction on the time step is somewhat relaxed in comparison with the DS1 model, but the disagreement of X_R becomes larger. These results confirm that the present model is a practically useful SGS model which satisfies both accuracy and computational stability.

3. 3 Flow around a circular cylinder

We have also applied the present model to the flow around a circular cylinder ($Re = 10{,}000$).[9] In the S model, C_S is set to 0.1 (S1 model) and 0.15 (S2 model). The former is the same value as in the previous test cases, while the latter is commonly used in outer flow calculations.

The calculated drag coefficient, C_D , which is the most important characteristic of bluff bodies, the root mean square of lift coefficient fluctuation, C_{Lrms} , and the time step allowing a stable calculation are shown in **Table 2**. The present model predicts the C_D in best agreement with the experimental data, while the DS model shows less accuracy and less

Table 1 Flow reattachment length in backward-facing step flow and computational time step.

	X_R/H	Δt
Present	6.44	4×10^{-4}
S-VD	6.40	4×10^{-4}
DS1($\gamma=\sqrt{3}$)	6.25	1×10^{-4}
DS2($\gamma=\sqrt{6}$)	6.06	2×10^{-4}
Exp.	6.51	–

computational stability. The S1 model underpredicts the C_D, while the present model predicts it accurately, although the same model parameter as in the previous test cases is used. Thus, the present model is considered to be more universal than the Smagorinsky model.

Figure 3 shows the mean velocity and velocity fluctuation distributions along the vertical line one diameter behind the cylinder center. The results given from a quasi-direct simulation (Q-DNS) using the QUICK scheme, which has been widely used in engineering applications, show less accuracy than those obtained by LES using any SGS model, especially in the turbulent quantity. The use of LES improves the prediction accuracy remarkably in engineering applications.

Table 2 Fluid force on circular cylinder and computational time step.

	C_D	C_{Lrms}	Δt
Present	1.17	0.44	4×10^{-3}
S1($Cs=0.1$)	1.32	0.61	4×10^{-3}
S2($Cs=0.15$)	1.19	0.39	4×10^{-3}
DS	1.08	0.39	2×10^{-3}
Q-DNS	1.00	0.10	4×10^{-3}
Exp.	1.1–1.2	0.3–0.5	–

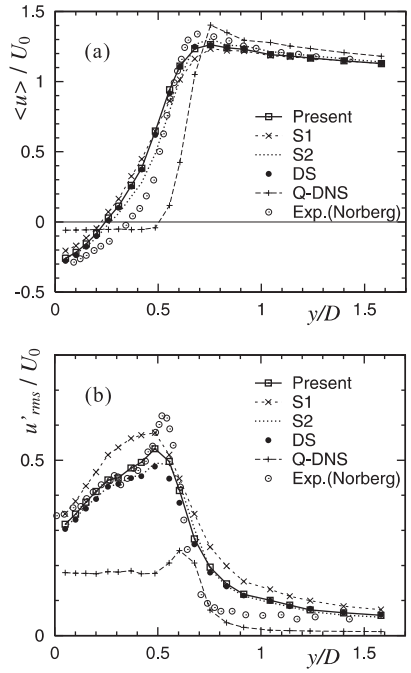

Fig. 3 Comparison of results of flow around a circular cylinder with experimental data: (a) mean streamwise velocity; (b) streamwise turbulent intensity.

4. Application to engineering-relevant problems

We applied the developed numerical method and SGS model to some engineering-relevant problems to assess the performance. Note that an artificial wall condition[10] assuming a three-layer wall function is applied at the wall surface.

4. 1 Flow around an Ahmed's bluff body

The three-dimensional flow around an Ahmed model (see **Fig. 4**) is a typical aerodynamic problem. We have conducted the calculations using a grid with 3.7 million grid points.[4] The rear slant angle of the body, θ, is set to 25°, and the incoming flow velocity is 40 m/s.

Table 3 shows the calculated C_D and the time step allowing a stable calculation. The C_D obtained using the present model agrees well with the experimental result, while the results using the DS model continue

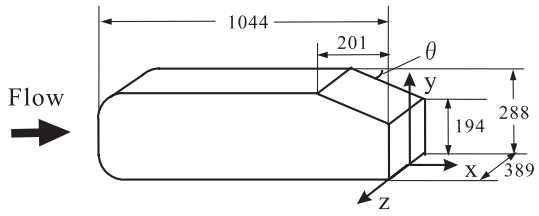

Fig. 4 Ahmed body and coordinate system.

Table 3 Drag coefficient of Ahmed body and computational time step.

	C_D (Error %)	Δt
Present	0.289 (2)	5×10^{-5}
DS	0.262 (7)	2.5×10^{-5}
Q-DNS	0.328 (16)	1×10^{-4}
Exp.	0.283	–

to show less accuracy and less computational stability. As for Q-DNS, the computational error in C_D is the largest: about 16%. **Figure 5** shows the mean velocity and the velocity fluctuation distributions in the symmetry plane. The agreement between the computational results using the present model and the experimental data[11] is quite satisfactory. The DS model predicts shorter separation length over the rear slant face, while Q-DNS does longer separation. These discrepancies result in the disagreement of C_D. Thus, the present model can be expected to work well in various three-dimensional engineering applications.

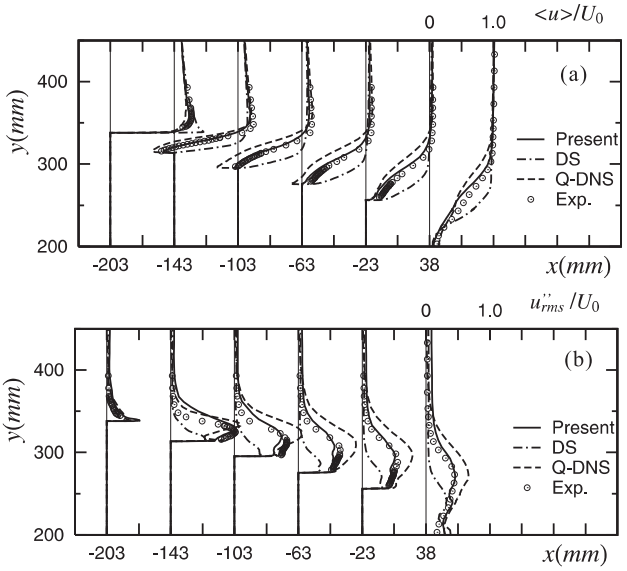

Fig. 5 Comparison of results of flow around an Ahmed body in symmetry plane: (a) mean streamwise velocity; (b) streamwise turbulent intensity.

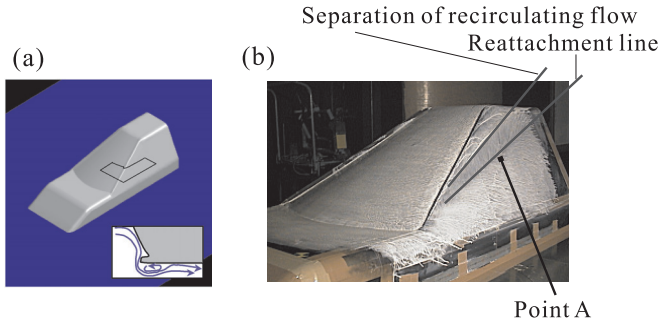

Fig. 6 Flow around a simplified front-pillar model: (a) appearance of a simplified front-pillar model; (b) oilflow pattern in the experiment and the characteristic lines.

4. 2 Wind noise generated from a simplified front-pillar model

Wind noise from the front-pillar is one of the greatest problems associated with automobiles. We have applied the present method to the flow around a simplified front-pillar model, as shown in **Fig. 6**.[9] The body height is 0.606 m, and the incoming flow velocity is 27.8 m/s. Three different grid resolutions (Grid 1-3) are used to examine the grid dependency. The maximum number of grid points is about 4.4 million. The corresponding experiments were performed in the RTRI's low-noise wind tunnel by Ichinose et al. (Toyota Motor Corporation). The wall-pressure fluctuation, which is a pseudo noise source according to Lighthill-Curle's theory, was measured on the surface of the side window.

First of all, the dynamic Smagorinsky model does not maintain a stable computation, even by setting the time step to one-forth that in the calculation for the present model. Therefore, all of the LES results shown in the following are those obtained using the present model.

Figure 7 shows the spectra of wall-pressure fluctuations on a reattachment point (see Fig. 6, point A). The experimental data demonstrate that the wall-pressure fluctuation has a wide-range spectrum. Although both LES and Q-DNS give insufficient results in the high-frequency range even when using the highest grid resolution (Grid 3), the

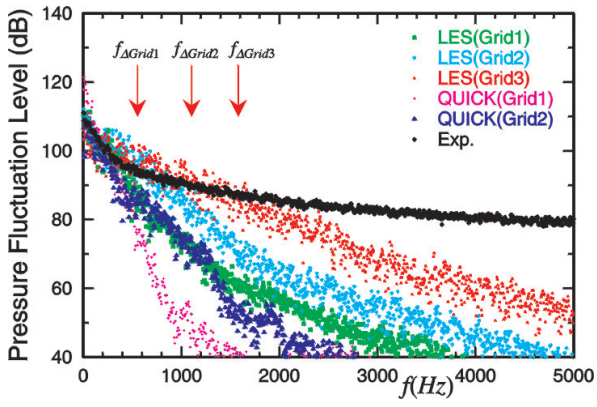

Fig. 7 Comparison of spectrum of wall-pressure fluctuation at point A.

results of LES show better agreement with the experimental data than those of Q-DNS in the high-frequency range. Using a lower grid resolution (Grid 1), the disagreement with the experimental data is seen from the lower frequency ranges in both results. In Fig. 7, f_Δ is a roughly estimated frequency equivalent to the cut-off wave number on the assumption of frozen turbulence:

$$f_\Delta = U_C / \left(2\pi\overline{\Delta}_1\right) \quad \cdots\cdots\cdots\cdots\cdots (12)$$

where U_C is set to half of the inflow velocity since the vortices generating in shear layers ordinarily convect with about half of the velocity difference of the shear flow, and $\overline{\Delta}_1$ is the filter width next to the wall. Theoretically, the computation cannot predict the frequency range higher than f_Δ. The estimated f_Δ for each grid almost corresponds to the frequency where the result of LES begins to decline in comparison with the experimental data, so that it can be said that the present LES fully utilizes the given grid resolution. According to an estimation,[9] LES can be expected to reduce the computational cost by more than 80% in comparison with Q-DNS.

5. Conclusions

We have proposed a new SGS model and discretization method. Constructed with the concept of mixed time scale, the proposed SGS model enables us to use a set of fixed model-parameters and to dispense with a wall-damping function of the van Driest's type. The accuracy of the present model is as good as that of the Smagorinsky model with the model parameter intentionally optimized for the relevant flow field and is higher than the dynamic Smagorinsky model. The usage of fixed model-parameters provides computational stability in contrast to the dynamic Smagorinsky model. Thus, the present model is a refined SGS model suited for engineering-relevant practical LES. On the other hand, the developed discretization method makes it possible to perform LES calculations in curvilinear grids with high stability and accuracy.

In addition, by comparing LES results with those given by Q-DNS, the effectiveness of LES is confirmed. The use of LES with the present model, instead of with Q-DNS, improves the prediction accuracy in both aerodynamic and aerodynamic noise analyses. Furthermore, LES is expected to become a practical tool for analyzing the complex turbulent flows including heat and mass transfer, chemical reaction, and combustion.

References

1) Piomelli, U., et al. : "Models for large eddy simulations of turbulent channel flows including transpiration," Report TF-32, Dep. of Mech. Eng., Stanford Univ. (1987)
2) Germano, M., et al. : "A dynamic subgrid-scale eddy viscosity model," Phys. Fluids, A**3**-7(1991), 1760
3) Inagaki, M., et al. : "A mixed-time-scale SGS model for practical LES," Trans. Jpn. Soc. Mech. Eng. : Ser. B, **68**(2002), 2572
4) Inagaki, M., et al. : Engineering Turbulence Modelling and Experiments 5, (2002), 257, Elsevier
5) Bardina, J., et al. : "Improved turbulence models based on large eddy simulation of homogenous, incompressible, turbulent flows," Report TF-10, Thermosciences Div., Dep. of Mech. Eng., Stanford Univ., (1983)
6) Inagaki, M. and Abe, K. : "An improvement of prediction accuracy of large eddy simulation on colocated grids," Trans. Jpn. Soc. Mech. Eng. : Ser. B, **64**(1998), 1981
7) Rhie, C. M. and Chow, W. L. : "Numerical study of the turbulent flow past an airfoil with trailing edge separation," AIAA J., **21**(1983), 1525
8) Kasagi, N. and Matsunaga, A. : "Three-dimensional particle-tracking velocimetry measurement of turbulence statistics and energy budget in a backward-facing step flow," Int. J. Heat and Fluid Flow, **16**(1995), 477
9) Inagaki, M. et al. : "Predictions of wall-pressure fluctuation in separated complex flows with improved LES and quasi-DNS," Proc. 3rd Int. Symp. on Turbulence and Shear Flow Phenomena, (2003), 941
10) Inagaki, M., et al. : "Numerical prediction of fluid-resonant oscillation at low Mach number," AIAA J., **40**(2002), 1823
11) Lienhart, H., et al. : "Flow and Turbulence Structures in the Wake of a Simplified Car Model (Ahmed Model)," DGLR Fach Symp. der AG STAB (2000), 15

(Report received on Jan. 15, 2004)

Masahide Inagaki
Year of birth : 1967
Division : Vehicle Dynamics Lab.
Research fields : Analysis of aero-dynamic noise, Computational fluid dynamics
Academic degree : Dr. Eng.
Academic society : The Jpn. Soc. of Mech. Eng., Jpn. Soc. of Fluid Mech.